Study of the Spatial Point Spread Function with Depth in Two-Photon Microscopy

Andrew Dunn, Vincent Wallace, Maria Coleno, Peter So*, Bruce Tromberg

Laser Medical and Microbeam Program (LAMMP)
Beckman Laser Institute
University of California at Irvine

*Dept of Mechanical Engineering, Massachusetts Institute of Technology

ABSTRACT

The spatial point spread function is studied for two-photon fluorescence imaging in turbid media. Using a Monte Carlo based model the effects of tissue optical properties on the point spread function, fluorescence generation, and fluorescence collection are studied. The simulated results are compared to measured point spread functions at different depths within a scattering sample. Results indicate that the limiting factor in two-photon imaging is a loss of signal caused by scattering rather than a loss of resolution.

Keywords: two-photon fluorescence, microscopy, Monte Carlo

1. INTRODUCTION

Recently two-photon fluorescence microscopy has showed promise for *in vivo* imaging of epithelial tissues.[1] Two-photon imaging produces depth resolved images due to the confinement of fluorescence generation to the focal volume of the microscope objective. For high numerical aperture microscope objectives this volume is on the order of a femtoliter. The confinement of the fluorescence to the focal region allows for efficient collection of the emitted light since the detected signal is not descanned. Another advantage of two-photon fluorescence over conventional fluorescence is that near-infrared light is used which penetrates more deeply into tissue due to decreased scattering.

While the penetration depth is deeper for two-photon fluorescence imaging than confocal imaging, the factors that influence this depth are not completely understood. In this paper, some of these factors are addressed through a model of two-photon fluorescence imaging in a turbid medium and measurements of fluorescent spheres embedded in a turbid medium.

2. MONTE CARLO MODEL

In order to study the effects of the tissue optical properties and beam parameters on the depth penetration of two-photon fluorescence imaging, a Monte Carlo based model was constructed. Monte Carlo models have been used extensively in the study of light propagation in tissue[2] and have been used to examine confocal imaging in turbid media.[3,4] In a Monte Carlo model individual photon trajectories are traced throughout the sample, where the average distance between interaction points is given by $1/\mu_t = 1/(\mu_s + \mu_a)$ where μ_s and μ_a are the scattering and absorption coefficients of the medium. The angular distribution of photon scattering is sampled from a Henyey-Greenstein[5] phase function, characterized by the average cosine of the scattering angle, g.

The geometry for the two-photon model is depicted in Figure 1 where the simulation consists of two parts. In the first part photons are traced in a focused beam geometry. The initial directions of the photons are chosen so that in the absence of scattering, the photon distribution in the region around the focus would be that of a diffraction limited spot. Photon paths were traced until the photon either exited the sample or was absorbed. Throughout the simulations, it was assumed that two-photon absorption did not significantly alter the photon distribution and therefore was neglected.

Send correspondence to Andrew Dunn, Beckman Laser Institute, 1002 Health Sciences Rd. East, University of California, Irvine, CA 92612 (adunn@bli.uci.edu)

Part of the SPIE Conference on Three-Dimensional and Multidimensional Microscopy: Image Acquisition and Processing VI • San Jose, California • January 1999
SPIE Vol. 3605 • 0277-786X/99/$10.00

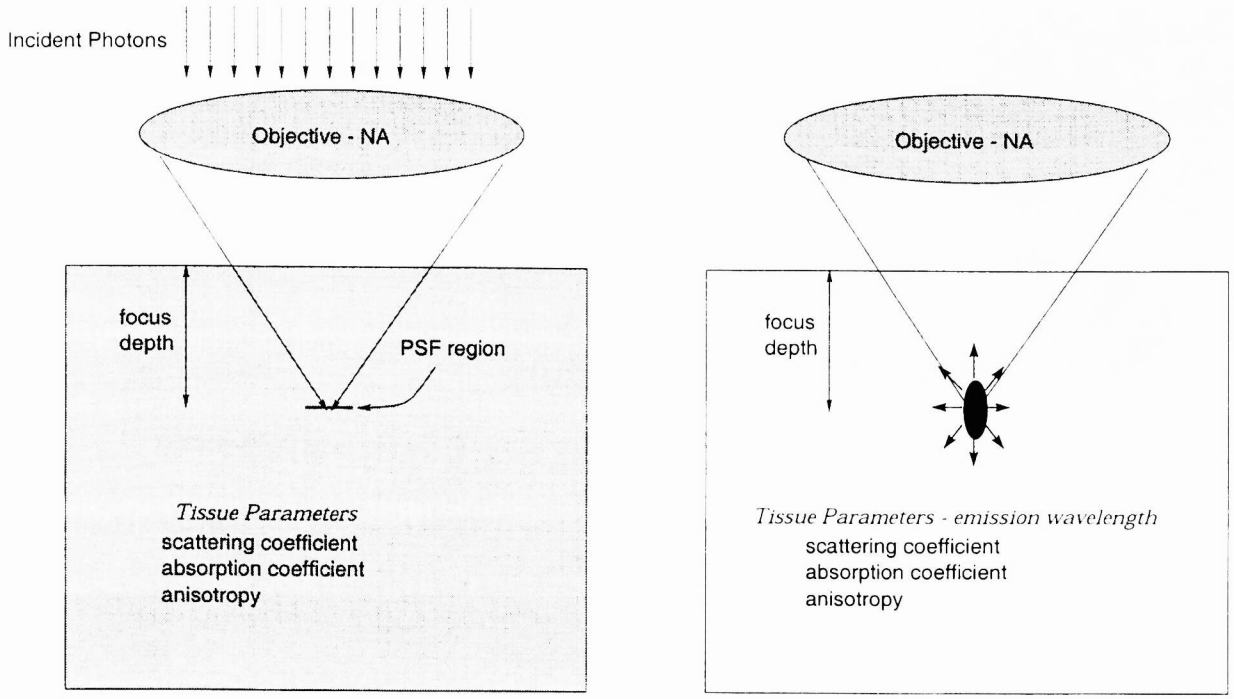

(a) excitation

(b) emission

Figure 1. Monte Carlo geometry demonstrating the two parts of the simulation.

Once all photons had been traced, the photon density $D(\mathbf{r}, t)$, at all points was computed. This quantity represented the spatial and temporal light distribution due to an infinitely short pulse. To compute the fluorescence generation due to a specified laser pulse, $D(\mathbf{r}, t)$ was convolved with the temporal laser pulse, $f(t)$, which was assumed to be Gaussian with a pulse width, τ. The spatial distribution of 2-photon fluorescence was then determined from

$$F_{ex}(\mathbf{r}) = \int \left| \int D(\mathbf{r}, t') f(t - t') dt' \right|^2 dt. \tag{1}$$

Equation (1) represents the integrated instantaneous intensity squared.

In the second half of the model, the generated fluorescence was propagated from within the tissue to determine the fraction of the generated two-photon fluorescence that is collected by the system. Fluorescent photons were launched isotropically from within the sample with a spatial distribution according to that computed in the first part of the model, $F_{ex}(\mathbf{r})$. Photons were traced until they exited the sample or were absorbed. For those photons exiting the sample, a geometrical ray trace was performed to determine whether the photon was collected by the objective.[3] The optical properties used in the second part were those at the shorter emission wavelength, which was typically assumed to be 500 nm.

The total detected fluorescence signal, S, was then calculated from the two parts of the model by integrating the product of the fluorescence generation and collection efficiency over the focal volume,

$$S = \frac{1}{2} \phi \eta \sigma \int C(\mathbf{r}) F_{ex}(\mathbf{r}) F_{em}(\mathbf{r}) d\mathbf{r} \tag{2}$$

where ϕ is the fluorescence quantum efficiency, η describes any losses in the collection optics and filters, σ is the two-photon absorption cross-section, $C(\mathbf{r})$ is the spatially distributed fluorophore concentration, and $F_{em}(\mathbf{r})$ is the fluorescence collection efficiency determined in the second half of the model.

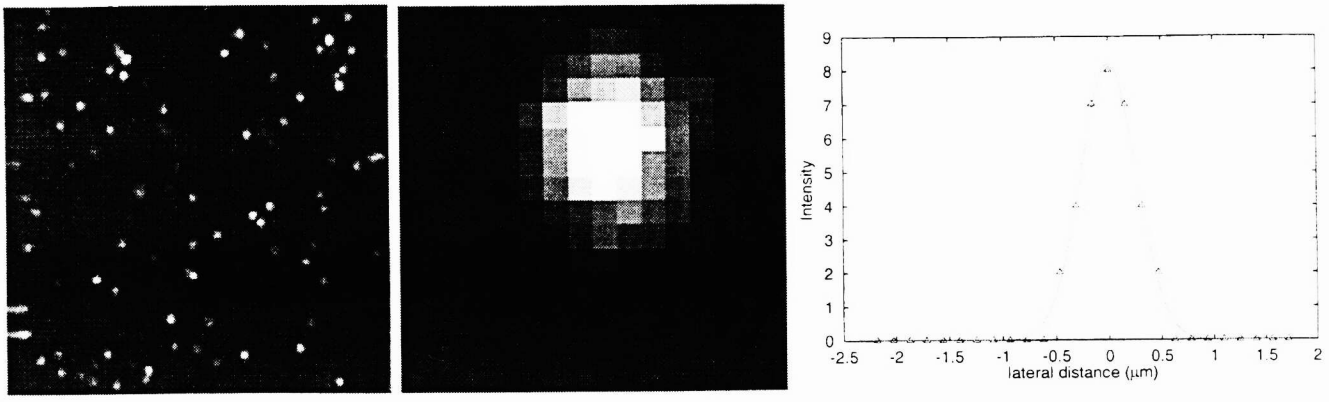

(a) entire image (b) single sphere (c) Gaussian fit

Figure 2. (a) Sample image of 0.1 μm spheres in 2% intralipid at a depth of 50 μm. (b) Example of a single sphere that was fit to a Gaussian function to determine its width (c).

3. EXPERIMENT

The two-photon microscope system consisted of an argon pumped titanium-sapphire laser (Coherent) tunable from 710-810 nm. The Ti:Sapphire laser produced 100 fs pulses at a repetition rate of 76 MHz. The laser was coupled to a Zeiss epifluorescent microscope through two orthogonal scan mirrors. The two-photon fluorescence signal was split between two photomultipliers so that one recorded fluorescent signals in the green region and the other in the red.

To measure the point spread function of the system, samples containing 0.1 μm diameter fluorescent spheres (BODIPY) were emebbded in a gelatin matrix with 2% intralipid to provide background scattering. Images were acquired at 20 μm intervals along the z axis. Each image was approximately 25 μm across with pixel dimensions of 256×256.

To determine the point spread function at a given depth, the xy image at that depth was analyzed as illustrated in Figure 2. In each of the xy images, individual spheres were analyzed. The individual spheres, shown in the middle of Figure 2 were fit to a Gaussian and the width of the Gaussian determined ($1/e^2$ width). Approximately 20 spheres at each image depth were averaged to determine the width of the point spread function as a function of focus depth.

4. RESULTS

4.1. Simulation

An example of the radial point spread function computed with the Monte Carlo model is shown in Figure 3. In this simulation the numerical aperture of the incident light was 1.3 and the sample had the following optical properties: $\mu_s = 100\,\mathrm{cm}^{-1}, \mu_a = 0.05\,\mathrm{cm}^{-1}$ and $g = 0.9$. The plots demonstrate the radial distribution of the fluorescence intensity at the focal plane and show that as the focal plane progresses deeper into the medium, the intensity of the generated fluorescence decreases.

To examine the effects of the scattering coefficient on both the generation and collection of two-photon fluorescence, simulations were run at scattering coefficients of 50, 100 and 150 cm^{-1}. The results are shown in Figure 4. The fluorescence generation results have been fit to an equation of the form $\exp(-a\mu_s^{\mathrm{ex}} z)$, where μ_s^{ex} is the scattering coefficient at the wavelength of the excitation light, z is the focus depth, and a is the fitting parameter. For the curves shown in Figure 4, $a = 2.6, 2.6$, and 2.5 for scattering coefficients of 50, 100 and 150 cm^{-1}, respectively.

The fraction of the generated photons that are collected by the objective is plotted in Figure 4 for the same set of scattering coefficients. This data was also fit to an exponential of the form $\exp(-b\mu_s^{\mathrm{em}} z)$, where μ_s^{em} is the scattering coefficient at the emission wavelength, z is the focus depth, and b is the fitting parameter. The fits yielded values of $b = 0.82, 0.75$, and 0.69 for the three scattering coefficients.

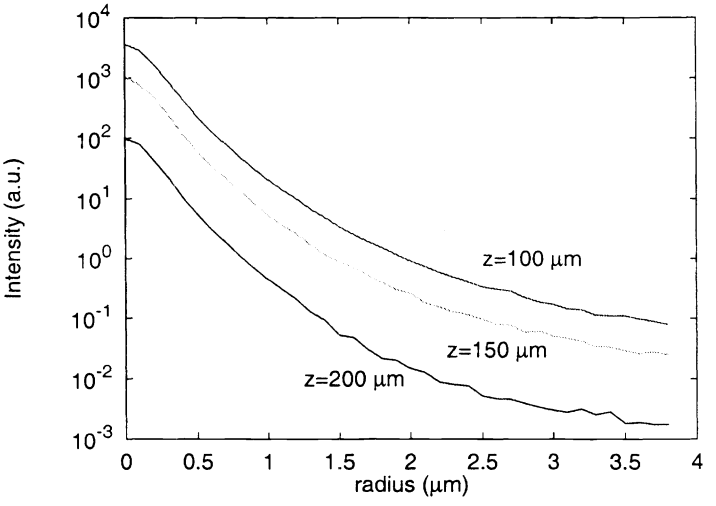

Figure 3. Example of computed radial point spread function at depths of 100, 150 and 200 μm.

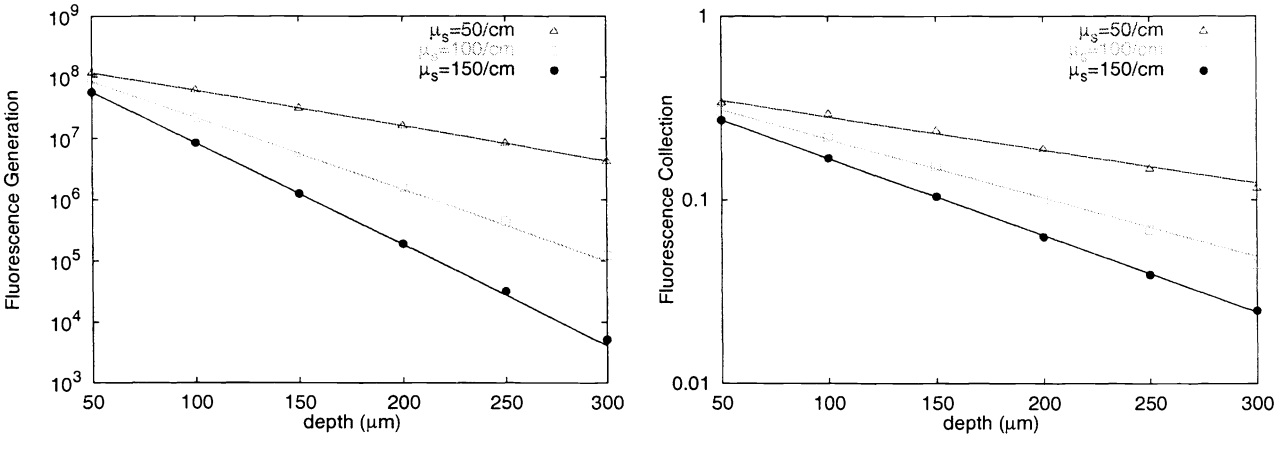

(a) fluorescence generation

(b) fluorescence collection

Figure 4. (a) Generation of fluorescence at increasing focal plane depths. (b) Collection fraction of the generated fluorescence.

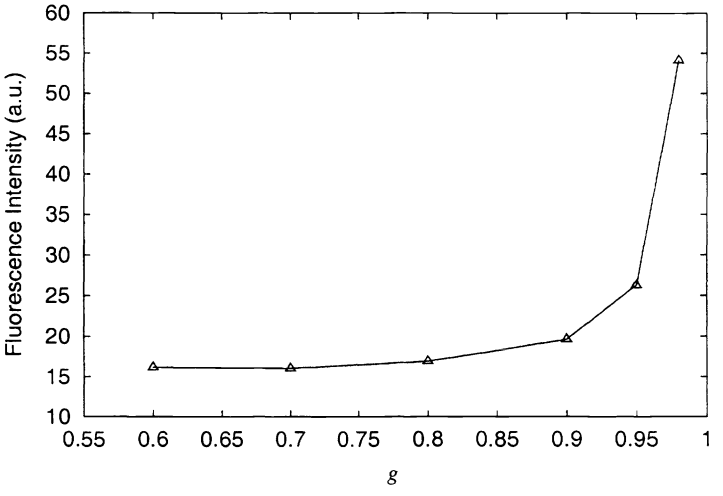

Figure 5. Two-photon fluorescence generation as a function of the anisotropy value, g.

Another parameter that is often important in determining the scattering properties of a turbid medium is the anisotropy factor, g which is equal to the average value of the cosine of the scattering angle. A value of 1 indicates complete forward scattering, while $g = 0$ represents isotropic scattering. To assess the impact of g on the generation of two-photon fluorescence, simulations were run with g varying between 0.6 and 0.98. The focus was located 200 μm beneath the surface in all cases and the scattering coefficient was held fixed at 100 cm^{-1}.

The generated fluorescence signal as a function of g is shown in Figure 5. The fluorescence intensity is relatively insensitive to g until g is larger than about 0.95. While typical values of g for tissues lie in the range of $0.8 - 0.95$,[6] g can be significantly higher in for single cells.[7] The large increase in the fluorescence generation at high values of g is due to the fact that for $g > 0.95$, photons can undergo a scattering event and still reach the focal region. However, when $g \leq 0.9$, the angular deviation of a photon trajectory is large enough to prevent that photon from reaching the focal region. Therefore, the generated fluorescence intensity is determined by single scattering for $g \leq 0.9$, whereas multiply scattered photons can contribute to the generation of fluorescence when $g > 0.95$.

4.2. Measurements

The measured width of the point spread function for the 0.1 μm spheres is plotted in Figure 6. The width remains relatively constant even to a depth of 250 μm. The mean value of 0.4 μm for the measured width is close to the theoretical width of 0.35 μm.[8] The lack of a significant decay in the measured width of the spheres indicates that the resolution of the microscope is not degraded to a depth of 250 μm.

The average signal strength from individual spheres is plotted in Figure 7 for each depth. The signal intensity was fit to an exponential decay and found to have a slope of 0.3. The measured decay represents the decay due to both fluorescence excitation and collection. The two factors cannot be separated in the experimental results as they are in the simulation.

4.3. Comparison of Measured and Simulated PSF

To compare the model to the measured results, the simulation was used to predict the generation and collection of fluorescence from a sample with optical properties identical to 2% intralipid. The optical properties of the intralipid at the excitation (800 nm) and emission wavelengths (515 nm) were: $\mu_s^{\text{ex}} = 60\,\text{cm}^{-1}$, $g^{\text{ex}} = 0.64$ and $\mu_s^{\text{em}} = 160\,\text{cm}^{-1}$, $g^{\text{em}} = 0.68$. The simulated results for the intralipid are shown in Figure 8 where the generation and collection efficiency are plotted in the upper graph.

The slopes of the exponential decay in the generation and collection were found to be 2.6 and 0.5, respectively. The total detected fluorescence signal is plotted in the lower graph in Figure 8 where the following values have been

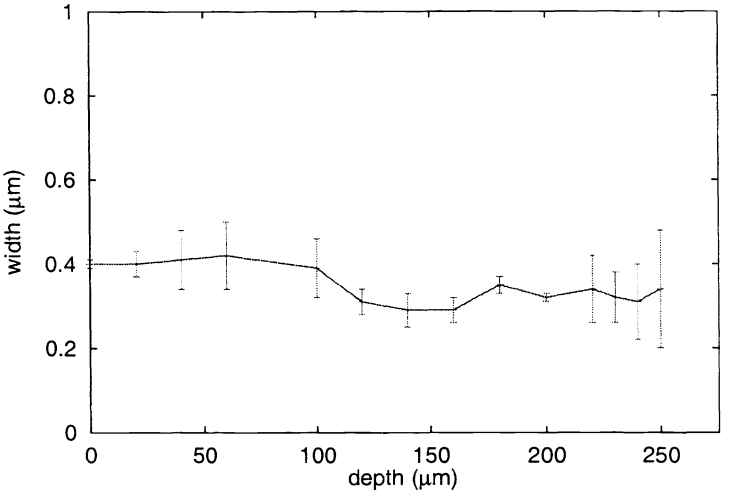

Figure 6. Measured width of 0.1 μm fluorescent spheres at increasing depth.

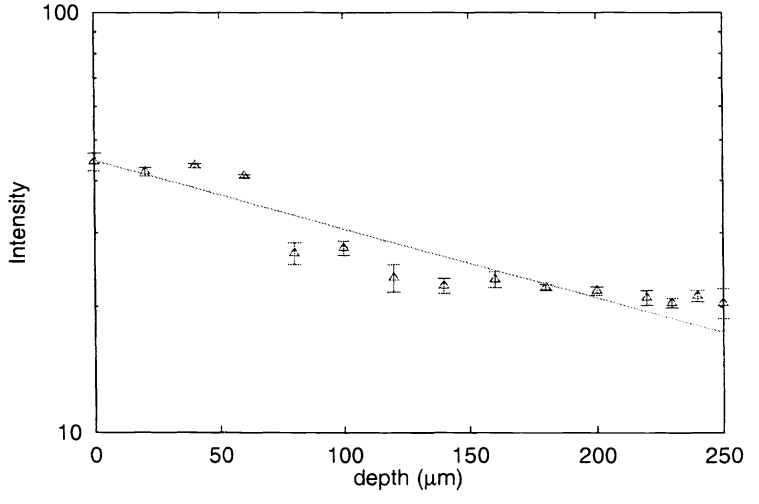

Figure 7. Measured signal intensity as a function of focus depth.

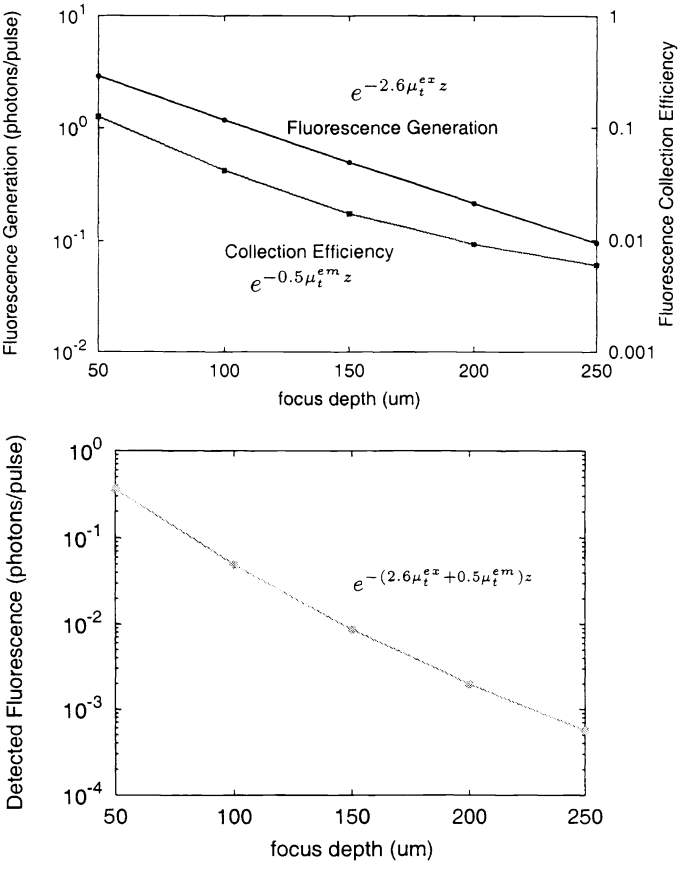

Figure 8. Simulated fluorescence generation and collection for 2% intralipid.

assumed: $\sigma = 10^{-48}$ cm^4 s/photon, $C = 10^{-5}$ M, $\phi = 0.4$, $\tau = 100$ fs, P_{avg}=1mW, NA=1.3, where τ is the pulse width and P_{avg} is the average power incident on the sample.

A comparison of the simulated and measured signal decay with depth indicates that a discrepancy exists in the slope of the decay. The measured decay curve is more gradual than the simulated decay. However, the fluorophores on the 0.1 μm spheres may be saturated at each laser pulse.[9] If the spheres are saturated, then the fluorescence generation is the same at all depths ($a = 0$), and the measured decay is due solely to the collection efficiency decay. In this case the comparison between the simulation and measurements should be based on the fit parameter for the collection efficiency, b. The simulation yields a value of 0.5 for b, while the measurements produce a value of 0.3. These values agree to within the errors associated with the measurements and the assumptions of the model.

5. CONCLUSIONS

This work has shown that the signal strength in two-photon fluorescence imaging in turbid media decays exponentially in a manner that depends on the optical properties at both the excitation and emission wavelengths. The primary factor that limits the maximum imaging depth is a loss of signal rather than a loss of resolution caused by a broadening of the point spread function. More work is required to quantify the complex relationship between the tissue optical properties and the experimental parameters.

ACKNOWLEDGMENTS

This work was supported by the National Institutes of Health under grants RR-01192 and GM-50958; the Office of Naval Research (ONR #N00014-91-C-0134), and the Department of Energy (DOE #DE-FG03-91ER61227).

REFERENCES

1. B. Masters, P. So, and E. Gratton, "Multiphoton excitation microscopy of *in vivo* human skin. functional and morphological optical biopsy based on three-dimensional imaging, lifetime measurements and fluorescence spectroscopy," *Annals of the New York Academy of Sciences* **838**, pp. 58–67, 1998.
2. S. Prahl, S. Jacques, and A. Welch, "A Monte Carlo model of light propagation in tissue," *SPIE* **IS 5**, pp. 102–111, 1989.
3. J. Schmitt, A. Knuttel, and M. Yadlowski, "Confocal microscopy in turbid media," *Journal of the Optical Society of America A* , pp. 2226–2235, 1994.
4. A. Dunn, C. Smithpeter, R. Richards-Kortum, and A.J. Welch, "Sources of contrast in confocal reflectance imaging," *Applied Optics* **35**, pp. 3441–3446, 1996.
5. L. Henyey and J. Greenstein, "Diffuse radiation in the galaxy," *Astrophys. Journal* **93**, pp. 70–83, 1941.
6. W. Cheong, S. Prahl, and A. Welch, "A review of the optical properties of biological tissue," *IEEE Journal of Quantum Electronics* **26**, pp. 2166–2185, 1990.
7. A. Dunn and R. Richards-Kortum, "Three-dimensional computation of light scattering from cells," *IEEE Journal of Special Topics in Quantum Electronics* **2**, pp. 898–905, 1997.
8. C. Sheppard and M. Gu, "Image formation in two-photon fluorescence microscopy," *Optik* **86**, pp. 104–106, 1990.
9. Z. Zhang, G. Sonek, H. Liang, M. Berns, and B. Tromberg, "Multiphoton fluorescence excitation in continuous-wave infrared optical traps," *Applied Optics* **37**, pp. 2766–2773, 1998.